Virus Research 335 (2023) 199195

Contents lists available at ScienceDirect

Virus Research

journal homepage: www.elsevier.com/locate/virusres

The neuropathological mechanism of EV-A71 infection attributes to inflammatory pyroptosis and viral replication via activating the hsa_circ_0045431/ hsa_miR_584/NLRP3 regulatory axis

Yajie Hu [a,b,#], Yue Yu [c,#], Ruian Yang [a,b], Ruibing Wang [a,b], Dandan Pu [a,b], Yujue Wang [a,b], Jingyuan Fan [a,b], Yunhui Zhang [a,b,*], Jie Song [c,*]

[a] Department of Respiratory Medicine, The First People's Hospital of Yunnan Province, Kunming, PR China
[b] The Affiliated Hospital of Kunming University of Science and Technology, Kunming, PR China
[c] Institute of Medical Biology, Chinese Academy of Medical Science and Peking Union Medical College, Yunnan Key Laboratory of Vaccine Research and Development on Severe Infectious Diseases, Kunming, PR China

ARTICLE INFO

Keywords:
Enterovirus A71 (EV-A71)
Pyroptosis
CircRNA
NLRP3

ABSTRACT

Neuropathological damage has been considered to be the main cause of death from EV-A71 infection, but the underlying mechanism has not been elucidated. Pyroptosis, a new form of inflammatory programmed cell death, has been verified to be involved in the pathogenesis of various viruses. circRNAs are a novel type of endogenous noncoding RNA gaining research interest in recent years, especially their special roles in the process of virus infection. Thus, in this study, we combined EV-A71, pyroptosis and circRNA to find a breakthrough in the pathogenesis of EV-A71 infection. Firstly, whether EV-A71 infection leaded to pyroptosis formation was examined by a series detection of cell death, cell viability, LDH release, caspase 1 activity, the expression levels of pyroptosis-related molecules and the concentrations of IL-1β and IL-18. Secondly, high-throughput sequencing of circRNAs was carried out to excavate the circRNA-miRNA-mRNA regulatory axis which might be associated with pyroptosis formation. Finally, the gain- and loss-of-functional experiments were further conducted to identify their functions. Our results showed that EV-A71 infection caused pyroptosis formation in SH-SY5Y cells. The circRNA sequencing analyzed the differentially expressed circRNAs and their possible functions. It was found that the hsa_circ_0045431/hsa_miR_584/NLRP3 regulatory axis might be involved in pyroptosis formation during EV-A71 infection. Then, hsa_circ_0045431 sponged hsa_miR_584 and hsa_miR_584 directly targeted NLRP3 were validated by IF, dual-luciferase, qRT-PCR and WB assays. Functional experiments were performed to further uncover that the up-regulation of hsa_circ_0045431 and NLRP3 promoted the inflammatory pyroptosis and viral replication, while the up-regulation of hsa_miR_584 suppressed the inflammatory pyroptosis and viral replication, and vice versa. Collectively, our study demystified that EV-A71 infection induced pyroptosis formation by activating hsa_circ_0045431/hsa_miR_584/NLRP3 regulatory axis, which could further effect viral replication. These findings provided novel insights into the pathogenesis of EV-A71 infection, and meanwhile revealed that the hsa_circ_0045431/ hsa_miR_584/NLRP3 regulatory axis can serve as a potential biological therapeutic target for EV-A71 infection.

1. Introduction

Hand, foot, and mouth disease (HFMD), a common viral illness usually affecting young children mostly younger than five years of age, is occurring more and more frequently throughout the western Pacific in areas such as Japan, Malaysia, Singapore, Thailand, and China (Saguil et al., 2019). It has been reported that HFMD is mainly caused by enterovirus 71 (EV-A71) and coxsackievirus A16 (CV-A16), or other subtypes CV-A6 or CV-A10 (Esposito and Principi, 2018). The common clinical manifestations are fever, rash, vomiting, headache, thereby most HFMD cases are mild, generally self-limiting, and have a good prognosis, but there were still severe cases with serious central nervous system

* Corresponding author.
E-mail addresses: zhangyh123kh@163.com (Y. Zhang), songjiekm@163.com (J. Song).
# These authors contributed equally to this work.

https://doi.org/10.1016/j.virusres.2023.199195
Received 22 May 2023; Received in revised form 17 July 2023; Accepted 8 August 2023

(CNS) complications, pulmonary edema and fatality, which was found to be mainly caused by EV-A71 infection (Chang et al., 2018). As a major cause of severe and fatal cases, EV-A71 infection has attracted more and more researchers' attention and is also growing to be a public health concern (Nayak et al., 2022). EV-A71, belonging to the *Picorvaviridae*, is a non-enveloped, positive, single-stranded RNA virus and four structural capsid proteins, including VP1, VP2 and VP3 on the external surface of the virion and VP4 within the interior of the viral particle (Solomon et al., 2010). To date, three inactivated monovalent EV-A71 vaccines were successfully licensed in 2016 in China, which showed high efficacy against EV-A71-associated HFMD, however, they all were no cross-protection against HFMD caused by other serotypes in children (Mao et al., 2016). Meanwhile, these inactivated monovalent EV-A71 vaccines didn't provide antiviral treatment for children who have already infected with EV-A71 (Yi et al., 2017). Thus, the exploration on EV-A71 is still rather important and necessary. Currently, the detailed pathogenesis of EV-A71-induced severe HFMD has not yet been clearly established, but a large number of studies have been demonstrated that aberrant expression of inflammatory cytokines, chemokines, and the balance of pro-inflammatory and anti-inflammatory cytokines contribute to the development of EV-A71 related severe HFMD (Zhang et al., 2020). Based on this point, our present study focused on the host inflammatory responses to EV-A71 infection to excavate the underlying mechanism for EV-A71-induced severe HFMD.

Pyroptosis is a new form of programmed cell death that relies on the activation of caspase-1 and is accompanied by the release of a large number of proinflammatory cytokines (Yu et al., 2021). Moreover, pyroptosis is closely linked with infectious disease occurrence, development, and immune regulation and plays an extremely important role in antagonizing and eliminating pathogenic infections and endogenous dangerous signals (Du et al., 2021). Currently, it was found that a large number of viruses could induce pyroptosis to varying degrees, which can be an effective defense against pathogen infection, on the other hand, excessive pyroptosis also can damage the host's health or aggravate disease progression (Man et al., 2017; Wang et al., 2022b). For example, efficient replication of the influenza A virus H7N9 virus in mouse lungs activates gasdermin E-mediated pyroptosis in alveolar epithelial cells, and that the released cytosolic contents then trigger a cytokine storm, which is closely linked to a poor prognosis and death (Wan et al., 2022). Human immunodeficiency virus (HIV) causes pyroptosis in $CD4^{+}T$ cells, leading to the release of inflammatory factors, which may involve the death of surrounding cells, giving rise to the death of additional $CD4^{+}T$ cells (Doitsh et al., 2014). Moreover, pyroptosis was also found to be involved in enteroviruses' infection (Wang et al., 2022b). For instance, AIM2 inflammasome-mediated pyroptosis in EV-A71-infected neuronal cells restricts viral replication (Yogarajah et al., 2017). Pyroptosis induced by EV-A71 and CV-B3 infection affects viral replication and host response (Wang et al., 2018b). Echovirus 11 infection induces pyroptotic cell death by facilitating NLRP3 inflammasome activation (Wang et al., 2022a). However, the detailed mechanism of pyroptosis during the process of EV-A71 infection is still unknown. This study aims to deeply excavate the potential mechanism of pyroptosis in regulating inflammatory response and viral replication caused by EV-A71.

2. Materials and methods

2.1. Cell culture, virus infection and transfection

The human neuroblastoma cell line SH-SY5Y were purchased from the American Type Culture Collection (ATCC, USA) and received incubation treatment in Dulbecco's Modified Eagle Medium (DMEM) (Gibco, USA) supplemented with 10% fetal bovine serum (FBS; HyClone, USA), penicillin (10,000 units/ml), and streptomycin (10,000 μg/ml) (Invitrogen, USA) in a humidified atmosphere containing 5% CO_2 at 37 °C. When the cells melted to about 80%, trypsin was added for digestion and passage. Logarithmic growth phase cells were taken for experiment.

For virus infection, cells were infected with EV-A71 strain (sub-genotype C4, GenBank: EU812515.1), which were isolated from an epidemic in Fuyang, China in 2008 at a multiplicity of infection (MOI) of 0.1. The cells were harvested at 0, 6, 12, 24, 48 and 72 h post infection (hpi). Cells infected with EV-A71 for 0 hpi were used as control.

For cell transfection, the overexpression and knockdown vectors of hsa-circ-0,045,431, miR-584 and NLRP3 and the corresponding negative control were generated from Genepharma (Shanghai, China). The above vectors were delivered into the SH-SY5Y cells by using Lipofectamine 3000 (Thermo Fisher, USA) following the manufactures' instructions for 48 h.

2.2. Immunofluorescence (IF) assay

The pre-cooled PBS was used to rinse the cells in 24-well plates (2×10^4 cells/well) for 3 times and 4% paraformaldehyde was employed to fix the cells deposited in plates of 24-well. After that, cells were subjected to permeabilization with PBS containing 0.1% Triton X-100 for 10 min at 37 °C. Then, 3% BSA was added for blockading the nonspecific binding. Next, the cells were incubated with the anti-VP1 (1:1000 dilution; Millipore, USA), anti-cleaved-Caspase1 (1:100 dilution; Affinity, USA) and anti-NLRP3 antibody (1:100 dilution; Affinity, USA) overnight at 4 °C, followed by incubation with fluorescein isothiocyanate (FITC)-conjugated donkey anti-mouse IgG and Daylight 594-conjugated donkey anti-rabbit IgG secondary antibodies (1:300 dilution; CST, USA) for 1 h. Finally, PBS was adopted to rinse the cells for 3 times and diamidino-2-phenylindole (DAPI; 1:1000 dilution; Beyotime, China) was taken to stain them at 37 °C for 5 min. With the help of a confocal fluorescence microscope (Leica, Germany), the images were obtained.

2.3. Quantitative reverse transcriptase polymerase chain reaction (qRT-PCR)

Cells were lysed in Trizol reagent (Tiangen, China) for the isolation of total RNA. However, for extraction of circRNA, the total RNA was needed to further treated with RNase R (epicenter, USA) for 10 min at 37 °C. Then, 500 ng of total RNA was reverse transcribed in a final volume of 10 μL with the Prime Script RT Master Mix (Takara, Japan). Finally, the relative expressions of circRNA, miRNA or genes were detected by using the SYBRR Green Master Mix (Takara, Japan) with a Step One Plus Real-Time PCR system (Applied Biosystems, USA). The specific primers of these examined genes were listed in Table S1. The glyceraldehyde-3-phosphatedehydrogenase (GAPDH) and U6 were regarded as internal controls and the $2^{-\Delta\Delta Ct}$ method was used to quantify the relative gene expression level.

2.4. Viral titer determination

The supernatants collected when SH-SY5Y cells showed maximal cytopathic effect from viral infection were used to viral titer examination with standard median cell culture infective doses (CCID50) assay. Vero cells were grown in 96-well cell culture plates to produce a confluent monolayer, and then washed with PBS, infected with 10-fold serially diluted supernatants, and incubated at 37 °C with 5% CO_2 for 3∼5 days. After incubation, the cells were fixed with 4% formaldehyde and stained with 1% crystal violet. Eventually, CCID50/1 ml values were calculated by the Reed-Muench method.

2.5. Flow cytometry assay for cell death

The Annexin V-FITC/Propidium iodide (PI) double staining kit (YEASEN, China) was employed to examine cell death in keeping with the protocol provided by the manufacturer. Briefly, the cells of different treated groups were harvested and resuspended into 500 μL binding buffer. Then, cells were incubated with Annexin V at 4 °C for 30 min in the dark and further stained with PI at room temperature for 5 min. Cells

were finally determined via flow cytometer (Agilent, China).

2.6. Cell proliferation assay

Cell Counting Kit-8 (CCK-8; Dojindo, Japan) was used to assess the cell proliferation. In general, 10 μl of CCK-8 solution was added to each plate and cells were incubated for 2 h. The cell viability was revealed by the optical density level which was detected through a microplate reader (Tecan, Switzerland) at 450 nm the absorbance which was measured at 450 nm. Proliferation rates were determined at 0, 6, 12, 24, 48 and 72 h after the abovementioned treatment.

2.7. Measurement of lactate dehydrogenase (LDH) release

LDH activity was measured using the LDH Cytotoxicity Assay Kit (Beyotime, China) according to the instructions provided by the manufacturer. The results are presented by percentage of maximum LDH release.

2.8. Detection of caspase1 activity

For the colorimetric method, caspase1 activity was determined using a Caspase1 Activity Assay Kit (Beyotime, China) following the recommended protocols. This assay is based on spectrophotometric detection of the chromophore ρ-nitroanilide (ρNA) after cleavage from the labeled substrate acetyl-Tyr-Val-Ala-Asp ρ-nitroanilide (Ac-YVAD-ρNA) by activated caspase-1. In brief, 50 μg protein was mixed with 20 nmol Ac-YVAD-ρNA in a 96-well microtiter plate and incubated for 2 h at 37 °C. The production of ρNA was monitored at 405 nm using a microplate reader.

2.9. Western blotting

The total proteins were collected from cells using radioimmunoprecipitation assay (RIPA) Lysis Buffer (Beyotime, China) with a cocktail of proteinase inhibitors (Roche Applied Science, Switzerland), and the protein concentration was detected with a BCA protein assay Kit (BioRad, USA), followed by denaturation at 98 °C for 10 min. After the separation by 10% sodium dodecyl sulfate-polyacrylamide gel electrophoresis (SDS-PAGE), the proteins were transferred onto polyvinylidene difluoride (PVDF) membranes (Millipore, USA) which were further blocked in 5% nonfat milk. Next, the membranes were immunoblotted with primary antibodies overnight at 4 °C and then hatched with the corresponding secondary antibodies for 1 h at room temperature after treated with ECL chemiluminescence kit (Beyotime, China). The antibodies included: anti-NLRP3 (1:1000 dilution; Affinity, USA), anti-ASC (1:2000 dilution; Affinity, USA), anti-Caspase 1 (1:1500 dilution; Affinity, USA), anti-Gasdermin D (1:1000 dilution; Affinity, USA), anti-IL-1β (1:800 dilution; Affinity, USA), anti-IL-18 (1:800 dilution; Affinity, USA), anti-VP1 (1:1000 dilution; China), anti-GAPDH (1:5000 dilution; CST, USA) and horseradish peroxidase (HRP)-conjugated goat anti-rabbit or -mouse secondary antibodies (1:2000 dilution; CST, USA). GAPDH functioned as a loading control. The gray value of blot was analyzed via Quantity One (BioRad, USA).

2.10. Evaluation of IL-1β and IL-8 protein levels by enzyme-linked immunosorbent assay (ELISA)

The concentrations of IL-1β and IL-8 in culture supernatants were used for ELISA detection quantified with commercial ELISA kits (Neobioscience, China) following the manufacturer's instructions. Sample absorbance values were read at 405 nm with a wavelength correction of 650 nm using a microplate reader (Tecan, China), and data analyzed using ESACalc software.

2.11. Flow cytometry for inflammatory cytokines examination

Twelve inflammatory cytokines, including TNF-α, IL-12, IL-4, IL-17, IL-8, IFN-γ, IL-10, IL-1β, IL-6, IL-2, IFN-α and IL-5, were examined by a Bio-Plex cytokine assay (RAISECARE, China) according to the instruction of a Bio-Plex cytokine assay (RAISECARE, China). Flow cytometric analysis was performed on a LEGENDplex v8.0 software.

2.12. High-throughput sequencing and data analysis

Total RNA was extracted from cells using Trizol reagent (TIANGEN, China) following the manufacturer's instructions. For enriching circRNAs, RNase R (epicenter, USA) was routinely applied to remove linear RNAs, while a Ribo-Zero™ Magnetic Kit (epicenter Technologies, USA) was used to remove ribosomal RNA (rRNA). Then, sequencing libraries were generated using an NEBNext Ultra RNA Library Prep Kit for Illumina (NEB, USA) as described in the previous study (Hu et al., 2021a, 2021b). Thereafter, based on the circRNA data obtained from sequencing, we screened the differentially expressed circRNAs, evaluated the genomic origin of circRNAs, identified the common differentially expressed circRNAs and found the up-regulated circRNAs among the common differentially expressed circRNAs. Meanwhile, it was also performed some bioinformatics analysis, including hierarchical clustering, functional classification and significant pathways of the differentially expressed circRNA parent genes, and construction of a circRNA-miRNA-mRNA coexpression network as illustrated in Fig. S1. Finally, according to the above analysis, we focused on the circRNA-miRNA-NLRP3 regulatory axis for following investigation.

2.13. Dual fluorescein reporter gene analysis

The wild-type (WT) sequence of hsa-circ-0,045,431 or NLRP3 untranslated region (UTR) containing miR-584 complementary sequence was inserted into pGL3-Basic vector (Promega, USA) to generate hsa-circ-0,045,431-WT and NLRP3-WT. The mutant-type (MUT) luciferase reporter vectors hsa-circ-0,045,431-MUT and NLRP3-MUT were formed based on the sequence containing mutant seeded site of miR-584. For luciferase reporter assay, 293T cells were co-transfected with miR-584 mimics or control and respective reporter plasmid using Lipofectamine 2000 (Invitrogen, USA). After incubation for 24 h, the luciferase activity was determined using the Dual Luciferase reporter 1000 Assay System (Promega, USA) and normalized to the Renilla luciferase activity.

2.14. Data analysis

The data from three independent experiments were presented as mean ± standard error of the mean (SEM). The software GraphPad Prism 7 was performed for statistical analysis. The significant difference was calculated by Student's *t*-test or one-way analysis of variance (ANOVA) with Tukey's post-hoc test. When the *P* value was less than 0.05, the difference was considered statistically significant.

3. Results

3.1. EV-A71 infection triggers cell death

The results of VP1 staining (Fig. S2A), virus copies (Fig. S2B) and virus titers (Fig. S2C) directly implied that EV-A71 was able to rapidly proliferate in SH-SY5Y cells with the extension of infection time. Cell death mechanisms are crucial for maintaining an optimal environment for proper cell function (D'Arcy, 2019). However, during viral infection, dysregulation of these systems can occur and contribute to disease pathogenetic mechanisms (Bertheloot et al., 2021). It was well-known that cell death contains many different styles, such as apoptosis, necroptosis, pyroptosis, autophagy, PANoptosis and so on (Bertheloot et al., 2021; D'Arcy, 2019). Our results found that with the time, the

percentage of Q3–1 (denoting late apoptotic cells or other dead cells), Q3–2 (denoting mid-apoptotic cells) and Q3–4 (denoting early apoptotic cells) were gradually increased (Fig. 1A), meanwhile the cell viability was declined over the time (Fig. 1B), which indicated that besides apoptosis, there were other cell death modes existed in EV-A71 infection. Moreover, the elevating LDH release directly pointed out that the types of cell death induced by EV-A71 infection were cell death modes of cell membrane destruction or increased permeability (Fig. 1C), which hinted that necroptosis and pyroptosis might be induced by EV-A71 infection. However, Caspase-1 activation plays a vital role in the activation of pyroptosis through cleavage of gasdermin D. Then, the caspase1 activity test further demonstrated that EV-A71 infection might be resulted in pyroptosis (Fig. 1D). Thus, these data confirmed that EV-A71 infection triggered cell death which probably included apoptosis and pyroptosis at the least.

3.2. EV-A71 infection induces pyroptosis formation

Pyroptosis is a form of lytic programmed cell death initiated by inflammasomes (such as NLRP3), which could detect both DNA and RNA viruses (Coll et al., 2022). This recruits the adaptor ASC complex and drives activation of caspase-1, which further cleaves gasdermin D and process pro-IL-1β and pro-IL18, and finally leads to mature IL-1β and IL-18 release via N-terminal of gasdermin D formed transmembrane pores (Huang et al., 2021). In this study, to assess whether EV-A71 infection induces pyroptosis formation, these molecules on the canonical pathway of pyroptosis were detected with a series of experiments. Firstly, the expressions of NLRP3, ASC, pro-Caspase1, cleaved Caspase 1, Gasdermin D, IL-1β and IL-18 mRNA and protein levels were examined by qRT-PCR and WB assays. The results found that EV-A71 infection significantly elevated the NLRP3, ASC, pro-Caspase1, cleaved Caspase1, Gasdermin D, IL-1β and IL-18 expressions over the time (Fig. 2A and 2B). Next, caspase dependence was a hallmark of different cell death styles, and Caspase-1 activated by Nod-like receptors (NLRs) forming the inflammasome is the beginning of pyroptosis; thereby Caspase1 was further tested. The IF picture was directly seen that the EV-A71-VP1 and cleaved Caspase1 were co-located in cytoplasm (Fig. 2C), which indicated that EV-A71 activated the formation of pyroptosis. Moreover, the final effector molecules IL-1β and IL-18 on the canonical pathway of pyroptosis were obviously secreted after EV-A71 infection in a time-dependent manner (Fig. 2D). Therefore, these data revealed that EV-A71 infection might induce pyroptosis formation.

3.3. EV-A71 infection activates inflammatory response

Pyroptosis is the process of inflammatory cell death (Yu et al., 2021). The primary function of pyroptosis is to induce strong inflammatory responses that defend the host against microbe infection; Excessive pyroptosis, however, leads to severe inflammatory damage (Kesavardhana et al., 2020). In the current study, we next examined whether EV-A71 infection caused strong inflammatory responses. It was seen that EV-A71 infection alters the expression of many inflammatory cytokines, especially IL-8, IL-1β and IL-6 (Fig. 3), and the expressions of IL-8, IL-1β and IL-6 also continued to increase with the extension of infection time (Table S2). Hence, this finding uncovered that EV-A71 infection might activate inflammatory response probably due to the pyroptosis formation induced by EV-A71.

3.4. circRNA may involve in pyroptosis progression induced by EV-A71 infection

Based on the above findings, we further hypothesized which upstream regulatory pathways contribute to pyroptosis formation induced by EV-A71 infection. Currently, accumulating evidences support the importance of ncRNA biology in the hallmarks of pyroptosis (Gao et al., 2022). Thus, we comprehensively analyzed the circRNA expression profile of EV-A71 infected SH-SY5Y cells, aiming to find out the key circRNA-miRNA-mRNA regulatory axis involved in pyroptosis pathway. As seen in Fig. 4, the differentially expressed circRNAs were distributed across the chromosomes, except the Y chromosome, and more than 90% of these circRNAs were transcribed from the exons of protein coding regions. Moreover, the hierarchical clustering analysis of these circRNAs revealed that differences in expression pattern of circRNAs from EV-A71 infected-cells at different time points (Fig. 5B). In order to find out the

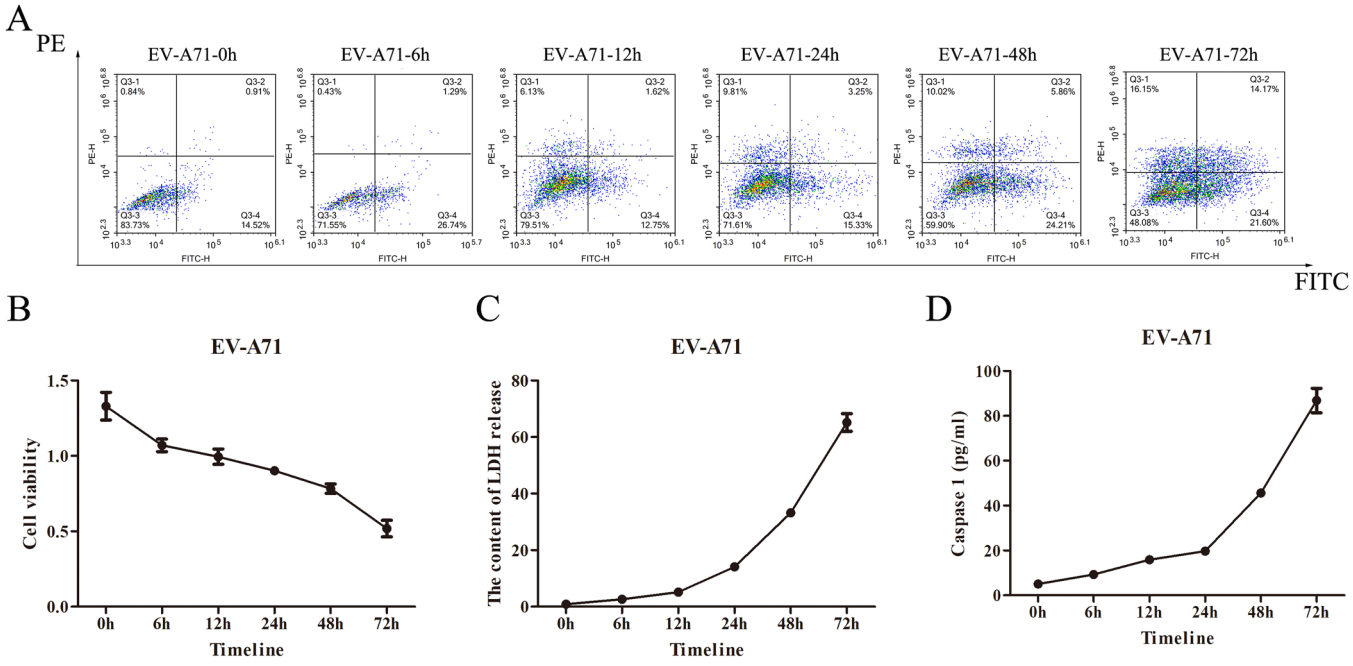

Fig. 1. EV-A71 infection triggers cell death of SH-SY5Y cells. (A) The percentage of cells undergoing cell death was calculated through Annexin V-FITC/PI double staining. (B) The cell viability was conducted with Cell Counting Kit-8. (C) Levels of LDH released into the cell culture medium from membrane pores were examined using an LDH Cytotoxicity Assay Kit. (D) Caspase1 activity was assessed with a Caspase1 Activity Assay Kit. .

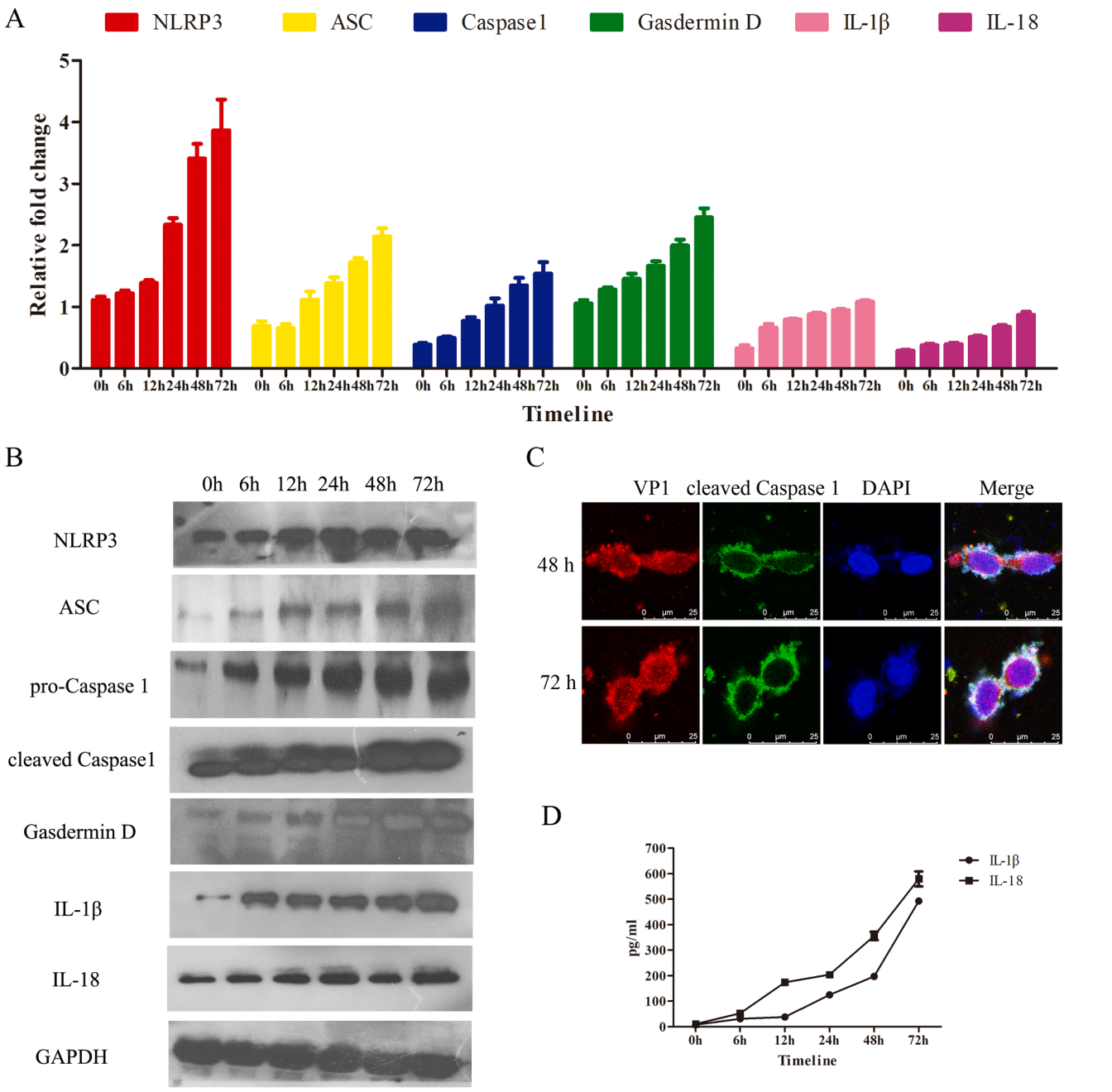

Fig. 2. EV-A71 infection induces NLRP3-dependent pyroptosis in SH-SY5Y cells. (A) NLRP3, ASC, Casepase1, Gasdermin D, IL-1β and IL-18 mRNA levels were analyzed by qRT-PCR. (B) The abundance of NLRP3, ASC, pro-Caspase1, cleaved Caspase 1, Gasdermin D, IL-1β and IL-18 was determined by WB analysis. (C) At 48 and 72 h post infection, infected SH-SY5Y cells were subjected to indirect immunofluorescence assays with anti-VP1 (red) and anti-Caspase-1 (green) antibodies. (D) Secretion of IL-1β and IL-18 upon infection with EV-A71 was measured with a commercial ELISA kit. .

key circRNAs, the up-regulated circRNAs during EV-A71 infection at both 24 hpi and 48 hpi draw our attention (Fig. 5A and 5C). Then, to further understand the potential functional implications of the circRNAs, the linear transcripts of the corresponding origination genes for circRNAs were annotated and further evaluated by GO and KEGG pathway analysis. The results showed that inflammatory response-related GO and KEGG were widely enriched, such as Interleukin-21 secretion, Positive regulation of NLRP3 inflammasome complex assembly, Interleukin-6 production, NOD-like receptor signaling pathway, Inflammatory mediator regulation of TRP channels, NF-kappa B signaling pathway, and Cytokine-cytokine receptor interaction (Fig. 6A and 6B). Meanwhile, the miRNA-related regulation was also highly enriched, such as Regulation of gene silencing by miRNA, miRNA catabolic process, miRNA metabolic process, miRNA loading onto RISC involved in gene silencing by miRNA, and Positive regulation of gene silencing by miRNA (Fig. 6A and 6B). Actually, growing evidence has reported that circRNAs could influence the gene expression targeted by miRNAs via sponging miRNAs (Kristensen et al., 2019). Thus, in this work, we found the circRNA-miRNA-NLRP regulatory axis which might be closely associated with pyroptosis (Fig. 6C and Table S3). And it was well-known that different pathogenic microorganisms may trigger different pyroptosis pathways (Tummers and Green, 2022). RNA viruses could activate NLPR3-mediated pyroptosis pathway (Fig. 6D), so EV-A71, as a single-stranded, positive-sense RNA virus, was hypothesized to activate the NLPR3-mediated pyroptosis pathway. Moreover, there has a literature recently been reported that

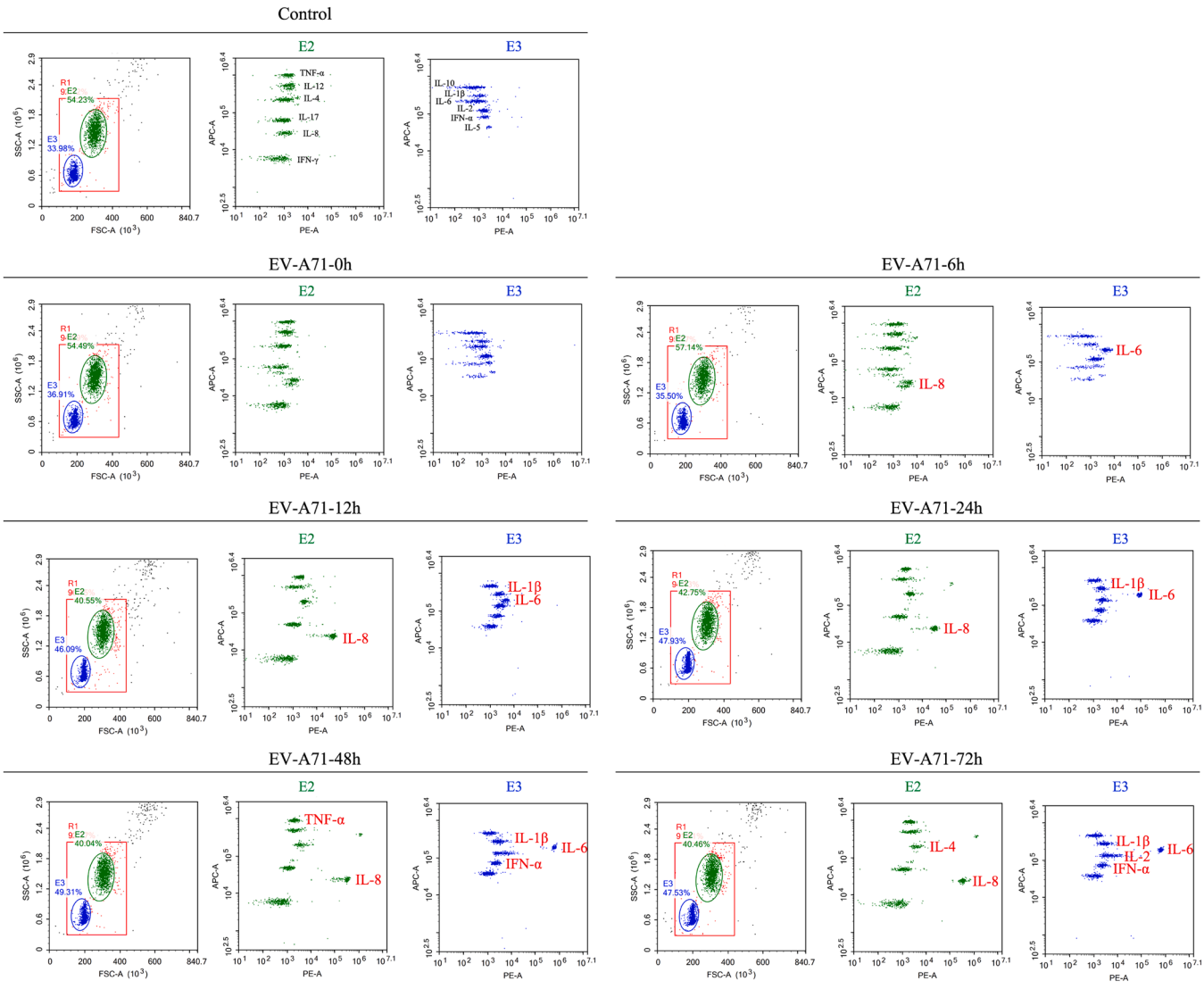

Fig. 3. EV-A71 infection activates the release of inflammatory cytokines. Flow cytometry results for 12 cytokines during EV-A71 infection. .

EV-A71 induced NLRP3 inflammasome in SH-SY5Y cells through miR-146a/CXCR4 axis (Guo et al., 2023), which further reinforced our suspicions.

3.5. hsa_circ_0045431, hsa_miR_584, NLRP3 are selected to be key factors participated in pyroptosis during EV-A71 infection

After we focused on NLRP3, we turned around and looked for its upstream miRNAs and circRNAs. It was seen that there were 10 circRNAs and 12 miRNAs implicated in regulation of NLRP3 (Fig. S3A). In order to clarify the accuracy of circRNA sequencing data and the actual expression of miRNA and NLRP3 regulated by these circRNAs, qRT-PCR was used to detect their expressions. It was found that the expressions of these circRNAs were basically consistent with circRNA sequencing data, except for has_circ_0128662 and has_circ_0084464 (Fig. S3B). However, the examined results of miRNAs showed that the expression level of hsa_miR_584 was significantly declined (Fig. S3C). Meanwhile, the NLPR3 expression was also evaluated gradually with time (Fig. S3D). Therefore, hsa_circ_0045431/hsa_miR_584/NLRP3 regulatory axis was chosen for following studies.

3.6. hsa_circ_0045431 promotes NLRP3 expressions through sponging miRNA-584

An increasing number of studies have reported that circRNAs act as miRNA sponges to regulate gene expression post-transcriptionally (Zhou et al., 2020); therefore, we investigated whether hsa_circ_0045431 has the ability to bind to hsa_miR_584 and then elevates NLRP3 expression. To identify the relationship of hsa_circ_0045431 and hsa_miR_584, the FISH assay and dual-luciferase report analysis were conducted in SH-SY5Y cells. FISH assay revealed that hsa_circ_0045431 and hsa_miR_584 were colocalized in the cytoplasm (Fig. S4A). Meanwhile, NLRP3 was also found to be expressed in cytoplasm (Fig. S4B). Then, a putative binding site in hsa_circ_0045431 for hsa_miR_584 were identified analyzing with https://circinteractome.nia.nih.gov/. And luciferase reporter assay revealed that the luciferase activity was evidently reduced by overexpression of hsa_miR_584 in hsa_circ_0045431-WT group, while it was not changed in hsa_circ_0045431-MUT group (Fig. S4C). Thus, based on these data, we hypothesized that hsa_miR_584 could be a target of hsa_circ_0045431.

In order to further study the regulatory mechanisms of hsa_miR_584, we performed target prediction by TargetScan (http://www.targetscan.org/vert_72/) and found the binding site of hsa_miR_584 in the 3′-UTR region of NLRP3 gene. Luciferase analysis indicated that over-expression

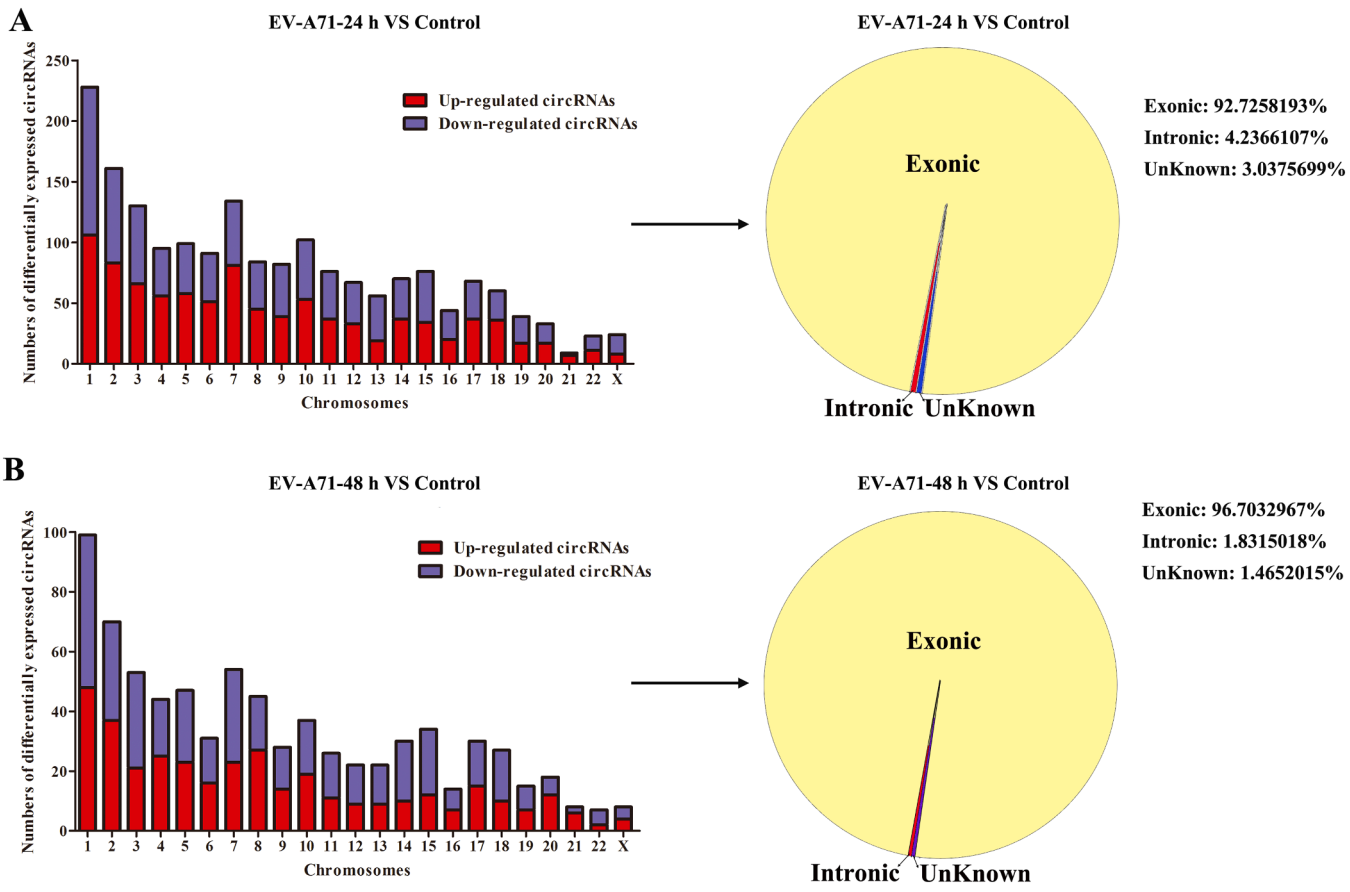

Fig. 4. Identification of differentially expressed circRNAs. (A) The number and genomic origin of differentially expressed circRNAs at 24 hpi with EV-A71 infection. (B) The number and genomic origin of differentially expressed circRNAs at 48 hpi with EV-A71 infection.

hsa_miR_584 in SH-SY5Y cells could effectively inhibit luciferase activity. However, no difference in luciferase activity could be seen in SH-SY5Y cells when we mutated the hsa_miR_584 binding site of NLRP3 (Fig. S4D). These data indicated that hsa_miR_584 could directly target NLRP3 and down-regulated NLRP3 expression. Therefore, the above results implied that hsa_circ_0045431 positively regulates NLRP3 expression by sponging hsa_miR_584.

3.7. hsa_circ_0045431/hsa_miR_584/NLRP3 regulatory axis accelerates pyroptosis formation and inflammatory storm caused by EV-A71 infection

To explore the potential influences of hsa_circ_0045431, hsa_miR_584 and NLRP3 on pyroptosis formation, the hsa_circ_0045431 overexpression and knockdown systems, hsa_miR_584 overexpression and knockdown systems, as well as NLRP3 overexpression and knockdown systems in SH-SY5Y cells were successfully established (Fig. S5). Firstly, we measured the cell viability through CCK8 assay. The data displayed that compared with EV-A71 infection, hsa_circ_0045431 overexpression, hsa_miR_584 inhibition and NLRP3 overexpression prior to EV-A71 infection evidently suppressed cell viability in SH-SY5Y cells, while hsa_circ_0045431 knockdown, hsa_miR_584 overexpression and NLRP3 silence prior to EV-A71 infection distinctly promoted cell viability in SH-SY5Y cells (Fig. 7A). Then, LDH release assay was used to detect the cytotoxicity. Compared to EV-A71 infection, hsa_circ_0045431 overexpression, hsa_miR_584 inhibition and NLRP3 overexpression in EV-A71-infected SH-SY5Y cells increased the LDH release, but hsa_circ_0045431 knockdown, hsa_miR_584 overexpression and NLRP3 silence in EV-A71-infected SH-SY5Y cells decreased the LDH release (Fig. 7B). Additionally, the caspase1 activity analysis disclosed that over-expression of hsa_circ_0045431 and NLRP3 or interference of hsa_miR_584 prior to EV-A71 infection led to higher caspase1 activity than EV-A71 infection. Nevertheless, the caspase1 activity was significantly lower in hsa_circ_0045431-downregulated, hsa_miR_584-upregulated and NLRP3-downregulated SH-SY5Y cells with EV-A71 infection than that in EV-A71-treated SH-SY5Y cells (Fig. 7C). Finally, we focused our analysis on the protein expression levels of NLRP3, ASC, pro-Caspase1, cleaved Caspase-1, Gasdermin D, IL-1β and IL-18. As expected, it was showed that forced hsa_circ_0045431 expression enhanced the expressions of the all above proteins, which was reversed by upregulating hsa_miR_584 and knocking down NLRP3 in EV-A71-infected SH-SY5Y cells. Meanwhile reduced hsa_circ_0045431 expression alleviated the increase of the above proteins expressions, which was also reversed by knocking down hsa_miR_584 and upregulating NLRP3 in EV-A71-infected SH-SY5Y cells (Fig. 8A). Moreover, the changed trends of IL-1β and IL-18 concentration resulted from ELISA examination were consistent with the WB results (Fig. 8B). Taken together, these results suggested that hsa_circ_0045431/hsa_miR_584/NLRP3 regulatory axis might accelerate pyroptosis formation in SH-SY5Y cells in respond to EV-A71 infection.

To further confirm the biological effects of hsa_circ_0045431/hsa_miR_584/NLRP3 regulatory axis on the induction of inflammatory responses during EV-A71 infection, flow cytometry was carried out to determine the expressions of inflammatory cytokines. Among these cytokines, the alterations of IL-8, IL-1β and IL-6 presented remarkably. The expressions of IL-8, IL-1β and IL-6 in EV-A71 group were basically higher than those in has-cic-0,045,431-Knockdown+EV-A71, miR-584-Over-+EV-A71 and NLRP3-Knockdown+EV-A71 groups, while basically lower than those in has-cic-0,045,431-Over+EV-A71, miR-584-Knockdown+EV-A71 and NLRP3-Over+EV-A71 groups (Fig. 9 and Table S4). Collectively, these findings indicated that the inhibition of the

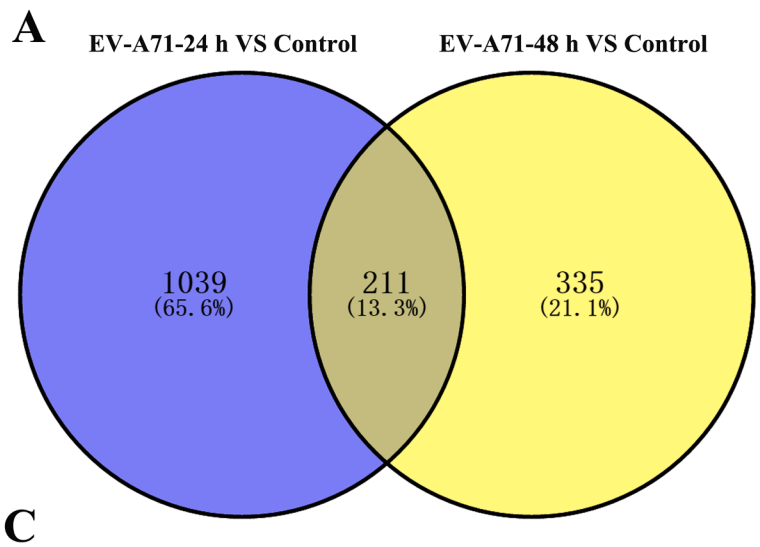

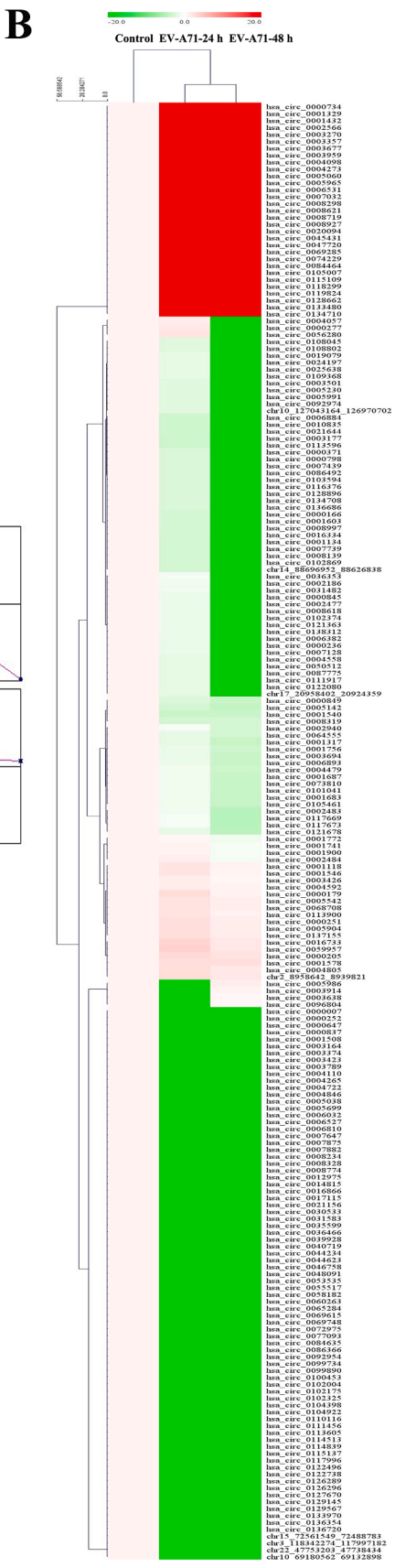

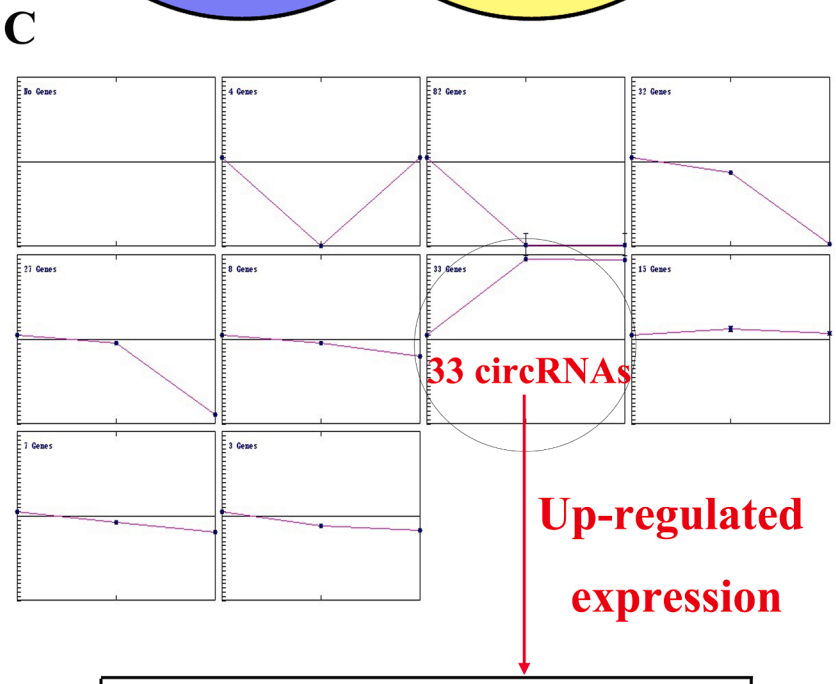

hsa_circ_0000205、hsa_circ_0000734、hsa_circ_0001329
hsa_circ_0001432、hsa_circ_0001578、hsa_circ_0002566
hsa_circ_0003270、hsa_circ_0003357、hsa_circ_0003677
hsa_circ_0003959、hsa_circ_0004098、hsa_circ_0004273
hsa_circ_0005060、hsa_circ_0005965、hsa_circ_0006531
hsa_circ_0007032、hsa_circ_0008298、hsa_circ_0008621
hsa_circ_0008719、hsa_circ_0008927、hsa_circ_0020094
hsa_circ_0045431、hsa_circ_0047720、hsa_circ_0069285
hsa_circ_0074229、hsa_circ_0084464、hsa_circ_0105007
hsa_circ_0115109、hsa_circ_0118299、hsa_circ_0119824
hsa_circ_0128662、hsa_circ_0133480、hsa_circ_0134710

Fig. 5. Specifical expression profiles of circRNAs induced by EV-A71 infection in SH-SY5Y cells. (A) Venn diagram displaying the common and differential circRNAs during EV-A71 infection at 24 hpi and 48 hpi. (B) Hierarchical cluster analysis of differentially expressed circRNAs between control and EV-A71-infected groups. (C) Trend analysis of 211 overlapping differentially expressed circRNAs.

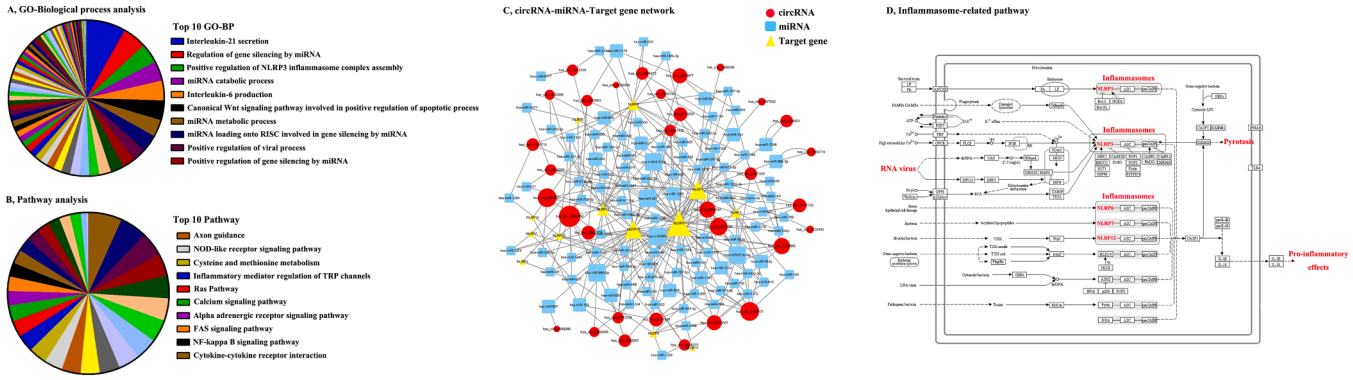

Fig. 6. Functional analysis of the persistently up-regulated circRNAs. (A) GO enrichment analysis for the parent genes of the persistently up-regulated circRNAs. (B) KEGG enrichment analysis for the parent genes of the persistently up-regulated circRNAs. (C) Construction of circRNA-medicated networks associated with NLRPs. (D) Bioinformatic analysis was performed to predict the interaction between pathogens and pyroptosis-related inflammatory pathway. .

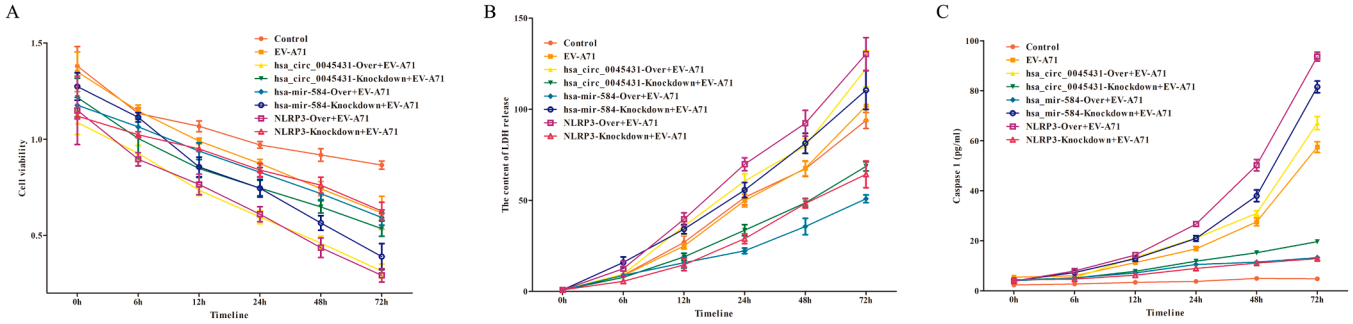

Fig. 7. has_circ_0045431/has-miR-584/NLRP3 regulatory axis involves in EV-A71-induced pyroptotic cell death. (A) The cell viability of SH-SY5Y cells was assessed by CCK8 kit. (B) The cell damage of SH-SY5Y cells was evaluated by LDH cytotoxicity assay kit. (C) The Caspase 1 activity of SH-SY5Y cells was examined by Caspase-1 activity assay kit. .

hsa_circ_0045431/hsa_miR_584/NLRP3 axis might weaken the inflammatory response resulted from EV-A71 infection, while overexpression of the hsa_circ_0045431/hsa_miR_584/NLRP3 axis might facilitate the inflammatory response caused by EV-A71 infection.

3.8. hsa_circ_0045431/hsa_miR_584/NLRP3 regulatory axis enhances viral replication

To address whether the hsa_circ_0045431/hsa_miR_584/NLRP3 regulatory axis could influence viral replication, the viral loads, virus titer and VP1 protein expression were further determined. It was observed that the up-regulation of hsa_circ_0045431 and NLRP3 or down-regulation of hsa_miR_584 increased the viral loads, virus titer and VP1 protein expression, but all these effects were reversed by the hsa_circ_0045431 and NLRP3 inhibition or hsa_miR_584 overexpression (Fig. 10). As a result, these data hinted that hsa_circ_0045431/hsa_miR_584/NLRP3 regulatory axis might play a driving role in EV-A71 infection.

4. Discussion

Recently, accumulating evidence has been demonstrated that inflammatory storm induced by EV-A71 infection is the main reason for accelerating the deterioration of EV-A71 infection, so researchers devotes more attention to the role of the inflammatory component to look for a consensus opinion about the pathogenesis of EV-A71 infection (Wang et al., 2012; Weng et al., 2010). However, pyroptosis happens to be a proinflammatory form of programmed cell death (Yu et al., 2021). It has been found that pyroptosis is important for host defense against invading viruses, and meanwhile involved in the pathogenic process of many viruses (Wang et al., 2022b). For example, Zika virus (ZIKV) induced adverse fetal outcomes via causing placental cell pyroptosis (Zhao et al., 2022). The pyroptosis caused by dengue virus (DENV) serotypes 1 and 2 and nonstructural protein 1 (NS1) could facilitate DENV replication in dermal fibroblasts (Wei et al., 2023). Influenza A virus H7N9 virus infection triggered lethal cytokine storm by activating gasdermin E-mediated pyroptosis of lung alveolar epithelial cells (Wan et al., 2022). In this study, we also found that EV-A71 infection could lead to the pyroptotic cell death of SH-SY5Y cells by activating NLRP3 inflammasome. Actually, growing evidence has been clearly pointed out that pyroptosis exerted an important role in EV-A71 infection (Wang et al., 2022b). For instance, EV-A71 infection induced gastric epithelial cells damage by triggering pyroptosis (Zhang et al., 2022). AIM2 inflammasome-mediated pyroptosis in EV-A71-infected neuronal cells restricts viral replication. Caspase-1, a critical molecule associated with pyroptosis, was activated in HeLa cells infected with EV-A71, which eventually resulted in a strong inflammatory response and meanwhile promoted viral replication (Yogarajah et al., 2017). Moreover, pyroptosis was also found to be involved in the molecular basis of viral pathogenesis of other enteroviruses, such as coxsackievirus B3 (Wang et al., 2018b), echovirus 11 (Wang et al., 2022a), etc. Thus, it is not surprising that EV-A71 infection induces pyroptosis in SH-SY5Y cells. And meanwhile we also found that EV-A71 infection activated an inflammatory response in SH-SY5Y cells, which was speculated that this may be caused by the formation of pyroptosis. However, it has not been clarified how the pyroptosis formation is regulated by EV-A71 infection. Numerous studies have shown that circRNAs could regulate the pyroptosis process by affecting the corresponding target genes (Gao et al., 2022). For example, hsa_circ_0001836 was discovered to up-regulate in glioma cells and its knockdown increased the expression of NLRP1

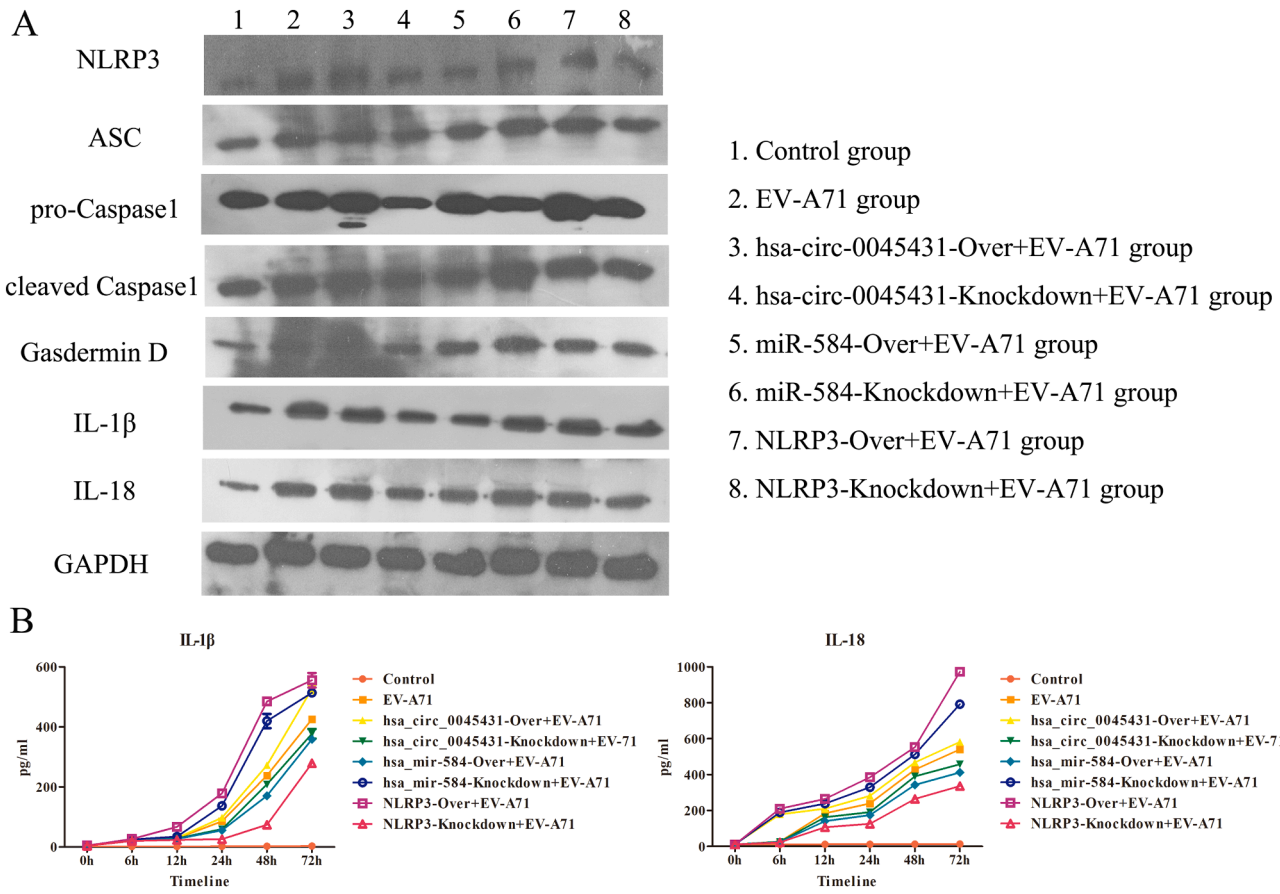

Fig. 8. has_circ_0045431/has-miR-584/NLRP3 regulatory axis promotes EV-A71-induced pyroptosis formation. (A) SH-SY5Y cells with different treatments were subjected to WB analysis for NLRP3, ASC, pro-Caspase1, cleaved Caspase 1, Gasdermin D, IL-1β and IL-18 expression. (B) The cell culture supernatant was subjected to the examination of ELISA for IL-1β and IL-18 concentration.

through DNA demethylation, thereby triggering cell pyroptosis, suggesting that hsa_circ_0001836 might be a potential therapeutic target for the treatment of glioma (Liu et al., 2021). CircHIPK3 promotes neuroinflammation through regulation of the miR-124–3p/STAT3/NLRP3 signaling pathway in Parkinson's disease (Zhang et al., 2023). circ-Katnal1 enhances inflammatory pyroptosis in sepsis induced liver injury through the miR-31–5p/GSDMD axis (Kang et al., 2022). Therefore, in this study, we focused our research on the regulation mechanism of pyroptosis on circRNAs. The analyzed results of circRNA sequencing presented that the linear transcripts of the corresponding origination genes for 33 up-regulated differentially expressed circRNAs were mainly enriched in inflammatory response-related GO or KEGG pathway, such as Interleukin-21 secretion, Positive regulation of NLRP3 inflammasome complex assembly, Interleukin-6 production, NOD-like receptor signaling pathway, Inflammatory mediator regulation of TRP channels, NF-kappa B signaling pathway, and Cytokine-cytokine receptor interaction. These results provided a good indication that circRNAs might be involved in the regulation of inflammatory responses during EV-A71 infection. However, pyroptosis is described to be a newly kind of pro-inflammatory programmed cell death (Kesavardhana et al., 2020). Hence, we linked circRNAs, inflammation and pyroptosis. Moreover, the execution of pyroptosis firstly depends on the formation of large cytosolic protein complexes termed inflammasomes, such as NLRP, AIM, etc. (Tsuchiya, 2020). Later, based on our results, we primarily paid our attention on NLRP-mediated pyroptosis pathway and the network of circRNA-miRNA-NLRP was constructed. It was seen that EV-A71 infection induced a complex circRNA regulatory network associated with NLRP. However, it has been reported that different NLRP family members can recognize different pathogens (Ohto, 2022). Our analyzed inflammasome-related pathway clearly indicated that RNA virus could be recognized by NLRP3, such as Newcastle disease virus (Gao et al., 2020), Zika virus (Wang et al., 2018a), HIV (He et al., 2020), et al. So we mainly focused on the circRNA regulatory network associated with NLRP3-dependent pyroptosis because EV-A71 is a human RNA virus. After screening and verification, we finally decided to explore the potential molecular mechanisms of hsa_circ_0045431/hsa_miR_584/NLRP3 regulatory axis in EV-A71 infection.

According to the above results, it was distinctly pointed out that EV-A71 could trigger significant changes of hsa_circ_0045431/hsa_miR_584/NLRP3 regulatory axis. Moreover, the luciferase reporter assay and bioinformatics tools also identified that hsa_circ_0045431 could act as a sponge of hsa_miR_584 and NLRP3 was the hsa_miR_584 direct target. Next, the overexpressed and knockdown vectors of hsa_circ_0045431, hsa_miR_584 and NLRP3 were purchased to conduct the gain- and loss-of functional experiments for their functions' examination. It was obviously showed that the up-regulation of hsa_circ_0045431/hsa_miR_584/NLRP3 regulatory axis facilitated pyroptosis formation and the production of inflammatory factors IL-1β and IL-18. Meanwhile, the inflammatory-related cytokines were examined to further observe the degree of inflammatory response. The results displayed that hsa_circ_0045431 and NLRP3 overexpression remarkably promoted the levels of inflammatory-related cytokines, but hsa_miR_584 overexpression markedly suppressed the increasing inflammatory-related cytokines. In recent years, neuroinflammation has always been identified as a major factor associated with the pathogenesis of HMFD, especially caused by EV-A71 infection (Heckenberg et al., 2022; Shah et al., 2020). Thus, these results suggested that hsa_circ_0045431 might enhance inflammatory pyroptosis during EV-A71 infection through

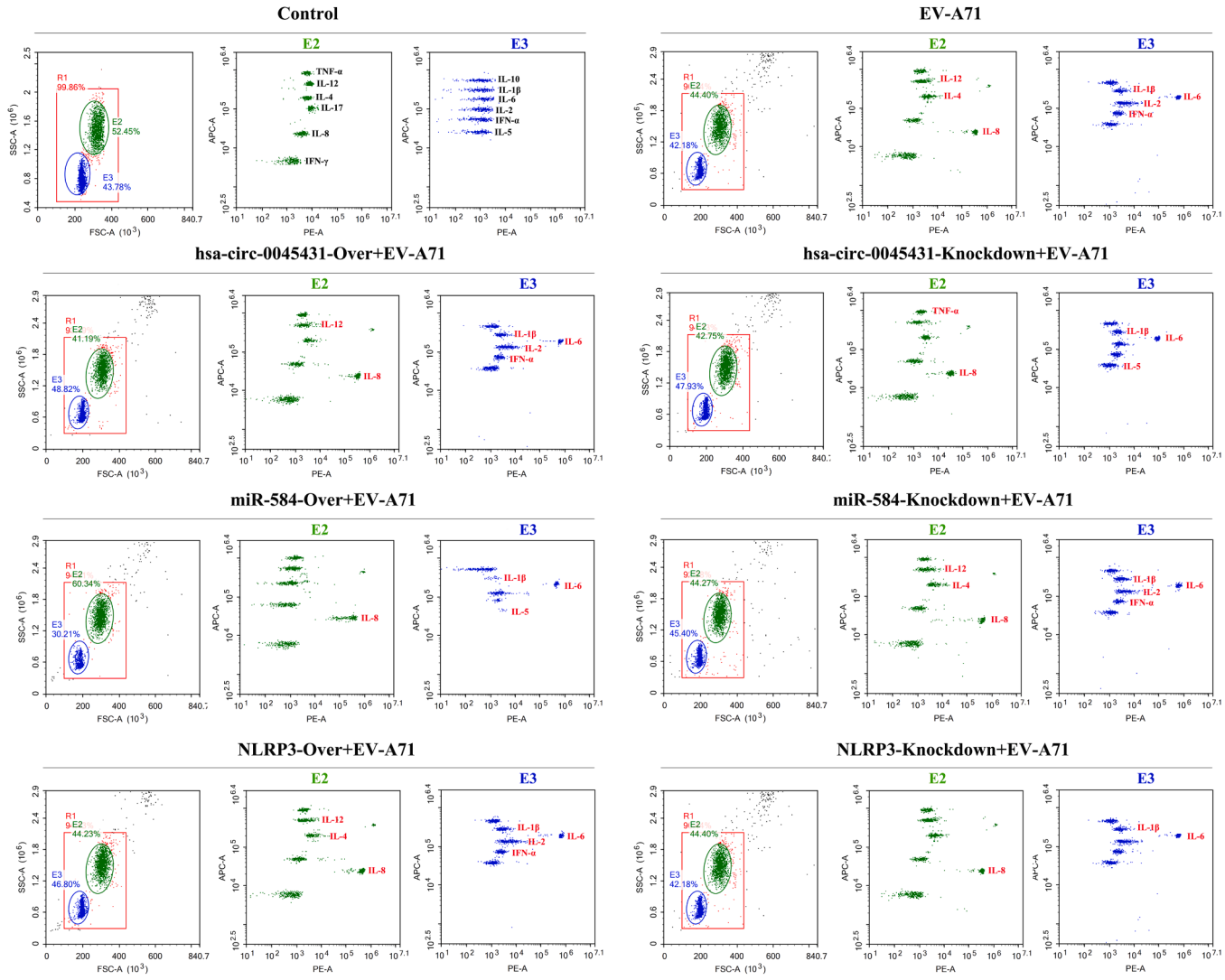

Fig. 9. has_circ_0045431/has-miR-584/NLRP3 regulatory axis enhances inflammatory response during EV-A71 infection. Flow cytometry analysis of TNF-α, IL-12, IL-4, IL-17, IL-8, IFN-γ, IL-10, IL-1β, IL-6, IL-2, IFN-α and IL-5 in SH-SY5Y cells with different plasmids transfection. .

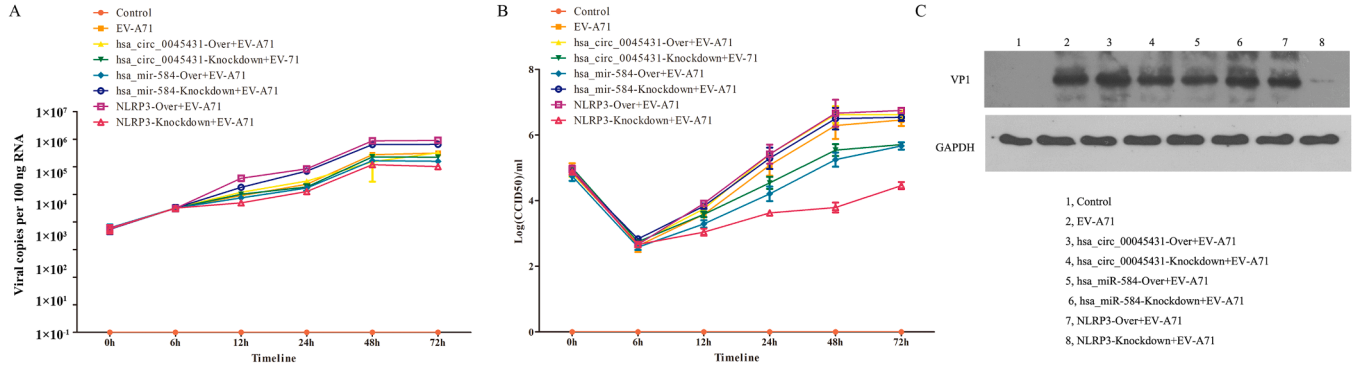

Fig. 10. The effect of has_circ_0045431/has-miR-584/NLRP3 regulatory axis on EV-A71 replication. (A) The viral genome copies of EV-A71 were determined by Taqman based qRT-PCR. (B) The virus titers of EV-A71 were evaluated with a plaque assay. (C) Cell lysates were prepared for WB to measure VP1 protein in treated SH-SY5Y cells.

sponging hsa_miR_584 and regulating NLRP3 expression. In addition, we further detected the role of hsa_circ_0045431/hsa_miR_584/NLRP3 regulatory axis in viral replication. In fact, during the EV-A71 infection of the central nervous system, excessive inflammatory response and neuronal cell death are considered as the key for the pathological damages, which mainly attributed to the virus's own replication and uncontrolled neuroinflammation (Shah et al., 2020; Wang et al., 2008). Our result was further uncovered that after overexpression hsa_circ_0045431 and NLRP3, the virus load, virus titer and VP1 expression were increased, but after inhibiting hsa_miR_584, these indicates were

also decreased, implying that hsa_circ_0045431/hsa_miR_584/NLRP3 regulatory axis might contribute to the viral replication. It is important to note here that we found evidence that infection by EV-A71 can occur through activation of the AIM2-mediated pyroptosis pathway, which restricts viral replication (Yogarajah et al., 2017). We also carefully analyzed the differences between our study and theirs, and found that their study adopted the SK-N-SH cells for EV-A71 infection with MOI=10 and they put their attention on AIM2, but our study used SH-SY5Y cell for EV-A71 infection with MOI=0.1 and we put our attention on NLRP3. Therefore, as long as the experimental conditions are different, it is not surprising that the experimental results are different. Furthermore, pyroptosis itself is a double-edged sword in the process of viral infection. Early in infection, the formation of pyroptosis prevents the damage caused by viral infection, but as pyroptosis continues to form, it can cause pathological damage to the host (Man et al., 2017; Wang et al., 2022b).

Taken together, our results demonstrated that EV-A71 infection could result in pyroptosis formation in SH-SY5Y cells. Subsequently, circRNA sequencing analysis revealed that the hsa_circ_0045431/hsa_miR_584/NLRP3 regulatory axis might be a key factor involved in pyroptosis formation during EV-A71 infection. And our following experiments further demonstrated that hsa_circ_0045431 indeed accelerated pyroptosis formation via modulating hsa_miR_584/NLRP3 signals in EV-A71-infected SH-SY5Y cells. Meanwhile, the activation of the hsa_circ_0045431/hsa_miR_584/NLRP3 regulatory axis could further promote viral replication in EV-A71-infected SH-SY5Y cells. Thus, these findings might not only make a more detailed understanding of EV-A71-induced inflammatory response mechanism, but also offer a new clue for clinical diagnosis targets of EV-A71 infection, as well as lay a foundation for the development of novel therapies to halt EV-A71.

CRediT authorship contribution statement

Yajie Hu: Conceptualization, Writing – original draft, Funding acquisition. **Yue Yu:** Methodology, Data curation. **Ruian Yang:** Software, Data curation. **Ruibing Wang:** Methodology, Software. **Dandan Pu:** Methodology. **Yujue Wang:** Visualization, Investigation. **Jingyuan Fan:** Software, Investigation. **Yunhui Zhang:** Conceptualization, Supervision, Writing – review & editing. **Jie Song:** Conceptualization, Writing – review & editing, Funding acquisition.

Declaration of Competing Interest

The authors declare that they have no known competing financial interests or personal relationships that could have appeared to influence the work reported in this paper.

Data availability

Data will be made available on request.

Acknowledgements

The present study was supported by funding from the National Natural Sciences Foundations of China (32000128), CAMS Innovation Fund for Medical Sciences (2021-I2M-1–043), Yunnan Applied Basic Research Projects (2019FB018, 202101AT070227 and 202201AT070237), Medical Reserve Talents of Yunnan Province Health and Family Planning (H-2019061), Kunming Medical University Joint special Project (202201AY070001–252), Top young talents of Yunnan province ten thousand talents plan (YNWR-QNBJ-2019–143 and XDYC-QNRC-2022–0300), Workstation of Academician Zhong Nanshan (202305AF150147) and Respiratory Diseases Clinical Medical Research Center of Yunnan Province (202102AA100057).

Supplementary materials

Supplementary material associated with this article can be found, in the online version, at doi:10.1016/j.virusres.2023.199195.

References

Bertheloot, D., Latz, E., Franklin, B.S., 2021. Necroptosis, pyroptosis and apoptosis: an intricate game of cell death. Cell Mol. Immunol. 18 (5), 1106–1121.
Chang, Y.K., Chen, K.H., Chen, K.T., 2018. Hand, foot and mouth disease and herpangina caused by enterovirus A71 infections: a review of enterovirus A71 molecular epidemiology, pathogenesis, and current vaccine development. Rev. Inst. Med. Trop. Sao Paulo 60, e70.
Coll, R.C., Schroder, K., Pelegrin, P., 2022. NLRP3 and pyroptosis blockers for treating inflammatory diseases. Trends Pharmacol. Sci. 43 (8), 653–668.
D'Arcy, M.S., 2019. Cell death: a review of the major forms of apoptosis, necrosis and autophagy. Cell Biol. Int. 43 (6), 582–592.
Doitsh, G., Galloway, N.L., Geng, X., Yang, Z., Monroe, K.M., Zepeda, O., Hunt, P.W., Hatano, H., Sowinski, S., Munoz-Arias, I., Greene, W.C., 2014. Cell death by pyroptosis drives CD4 T-cell depletion in HIV-1 infection. Nature 505 (7484), 509–514.
Du, T., Gao, J., Li, P., Wang, Y., Qi, Q., Liu, X., Li, J., Wang, C., Du, L., 2021. Pyroptosis, metabolism, and tumor immune microenvironment. Clin. Transl. Med. 11 (8), e492.
Esposito, S., Principi, N., 2018. Hand, foot and mouth disease: current knowledge on clinical manifestations, epidemiology, aetiology and prevention. Eur. J. Clin. Microbiol. Infect. Dis. 37 (3), 391–398.
Gao, L., Jiang, Z., Han, Y., Li, Y., Yang, X., 2022. Regulation of Pyroptosis by ncRNA: a Novel Research Direction. Front Cell Dev. Biol. 10, 840576.
Gao, P., Chen, L., Fan, L., Ren, J., Du, H., Sun, M., Li, Y., Xie, P., Lin, Q., Liao, M., Xu, C., Ning, Z., Ding, C., Xiang, B., Ren, T., 2020. Newcastle disease virus RNA-induced IL-1beta expression via the NLRP3/caspase-1 inflammasome. Vet. Res. 51 (1), 53.
Guo, H., Zhu, Y., Zou, Y., Li, C., Wang, Y., De, G., Lu, L., 2023. Enterovirus 71 induces pyroptosis of human neuroblastoma SH-SY5Y cells through miR-146a/CXCR4 axis. Heliyon 9 (4), e15014.
He, X., Yang, W., Zeng, Z., Wei, Y., Gao, J., Zhang, B., Li, L., Liu, L., Wan, Y., Zeng, Q., Gong, Z., Liu, L., Zhang, H., Li, Y., Yang, S., Hu, T., Wu, L., Masliah, E., Huang, S., Cao, H., 2020. NLRP3-dependent pyroptosis is required for HIV-1 gp120-induced neuropathology. Cell Mol. Immunol. 17 (3), 283–299.
Heckenberg, E., Steppe, J.T., Coyne, C.B., 2022. Enteroviruses: the role of receptors in viral pathogenesis. Adv. Virus Res. 113, 89–110.
Hu, Y., Xu, Y., Deng, X., Wang, R., Li, R., You, L., Song, J., Zhang, Y., 2021a. Comprehensive analysis of the circRNA expression profile and circRNA-miRNA-mRNA network in the pathogenesis of EV-A71 infection. Virus. Res. 303, 198502.
Hu, Y., Yang, R., Zhao, W., Liu, C., Tan, Y., Pu, D., Song, J., Zhang, Y., 2021b. circRNA expression patterns and circRNA-miRNA-mRNA networks during CV-A16 infection of SH-SY5Y cells. Arch. Virol. 166 (11), 3023–3035.
Huang, Y., Xu, W., Zhou, R., 2021. NLRP3 inflammasome activation and cell death. Cell Mol. Immunol. 18 (9), 2114–2127.
Kang, K., Li, N., Gao, Y., Wang, C., Chen, P., Meng, X., Yang, W., Zhao, M., Yu, K., 2022. circ-Katnal1 Enhances Inflammatory Pyroptosis in Sepsis-Induced Liver Injury through the miR-31-5p/GSDMD Axis. Mediat. Inflamm., 8950130
Kesavardhana, S., Malireddi, R.K.S., Kanneganti, T.D., 2020. Caspases in Cell Death, Inflammation, and Pyroptosis. Annu. Rev. Immunol. 38, 567–595.
Kristensen, L.S., Andersen, M.S., Stagsted, L.V.W., Ebbesen, K.K., Hansen, T.B., Kjems, J., 2019. The biogenesis, biology and characterization of circular RNAs. Nat. Rev. Genet. 20 (11), 675–691.
Liu, Y., Wu, H., Jing, J., Li, H., Dong, S., Meng, Q., 2021. Downregulation of hsa_circ_0001836 Induces Pyroptosis Cell Death in Glioma Cells via Epigenetically Upregulating NLRP1. Front Oncol. 11, 622727.
Man, S.M., Karki, R., Kanneganti, T.D., 2017. Molecular mechanisms and functions of pyroptosis, inflammatory caspases and inflammasomes in infectious diseases. Immunol. Rev. 277 (1), 61–75.
Mao, Q.Y., Wang, Y., Bian, L., Xu, M., Liang, Z., 2016. EV71 vaccine, a new tool to control outbreaks of hand, foot and mouth disease (HFMD). Expert Rev. Vaccines 15 (5), 599–606.
Nayak, G., Bhuyan, S.K., Bhuyan, R., Sahu, A., Kar, D., Kuanar, A., 2022. Global emergence of Enterovirus 71: a systematic review. Beni. Suef. Univ J. Basic Appl. Sci. 11 (1), 78.
Ohto, U., 2022. Activation and regulation mechanisms of NOD-like receptors based on structural biology. Front. Immunol. 13, 953530.
Saguil, A., Kane, S.F., Lauters, R., Mercado, M.G., 2019. Hand-Foot-and-Mouth Disease: rapid Evidence Review. Am. Fam. Physician 100 (7), 408–414.
Shah, J., Sijun, L., Hui, Z., Zeb, F., Haq, I.U., Ullah, A., 2020. Neurological Complications Of Hand, Foot And Mouth Disease In Children: a Review. J. Ayub Med. Coll. Abbottabad. 32 (4), 562–569.
Solomon, T., Lewthwaite, P., Perera, D., Cardosa, M.J., McMinn, P., Ooi, M.H., 2010. Virology, epidemiology, pathogenesis, and control of enterovirus 71. Lancet Infect. Dis. 10 (11), 778–790.
Tsuchiya, K., 2020. Inflammasome-associated cell death: pyroptosis, apoptosis, and physiological implications. Microbiol. Immunol. 64 (4), 252–269.
Tummers, B., Green, D.R., 2022. The evolution of regulated cell death pathways in animals and their evasion by pathogens. Physiol. Rev. 102 (1), 411–454.
Wan, X., Li, J., Wang, Y., Yu, X., He, X., Shi, J., Deng, G., Zeng, X., Tian, G., Li, Y., Jiang, Y., Guan, Y., Li, C., Shao, F., Chen, H., 2022. H7N9 virus infection triggers

lethal cytokine storm by activating gasdermin E-mediated pyroptosis of lung alveolar epithelial cells. Natl. Sci. Rev. 9 (1), nwab137.
Wang, C., Yang, R., Yang, F., Han, Y., Ren, Y., Xiong, X., Wang, X., Bi, Y., Li, L., Qiu, Y., Xu, Y., Zhou, X., 2022a. Echovirus 11 infection induces pyroptotic cell death by facilitating NLRP3 inflammasome activation. PLoS Pathog. 18 (8), e1010787.
Wang, S.M., Ho, T.S., Shen, C.F., Liu, C.C., 2008. Enterovirus 71, one virus and many stories. Pediatr. Neonatol. 49 (4), 113–115.
Wang, S.M., Lei, H.Y., Liu, C.C., 2012. Cytokine immunopathogenesis of enterovirus 71 brain stem encephalitis. Clin. Dev. Immunol. 2012, 876241.
Wang, W., Li, G., De, W., Luo, Z., Pan, P., Tian, M., Wang, Y., Xiao, F., Li, A., Wu, K., Liu, X., Rao, L., Liu, F., Liu, Y., Wu, J., 2018a. Zika virus infection induces host inflammatory responses by facilitating NLRP3 inflammasome assembly and interleukin-1beta secretion. Nat. Commun. 9 (1), 106.
Wang, Y., Qin, Y., Wang, T., Chen, Y., Lang, X., Zheng, J., Gao, S., Chen, S., Zhong, X., Mu, Y., Wu, X., Zhang, F., Zhao, W., Zhong, Z., 2018b. Pyroptosis induced by enterovirus 71 and coxsackievirus B3 infection affects viral replication and host response. Sci. Rep. 8 (1), 2887.
Wang, Z., Yu, H., Zhuang, W., Chen, J., Jiang, Y., Guo, Z., Huang, X., Liu, Q., 2022b. Cell pyroptosis in picornavirus and its potential for treating viral infection. J. Med. Virol. 94 (8), 3570–3580.
Wei, K.C., Wei, W.J., Liao, C.L., Chang, T.H., 2023. Discrepant activation pattern of inflammation and pyroptosis induced in dermal fibroblasts in response to dengue virus serotypes 1 and 2 and nonstructural protein 1. Microbiol. Spectr. 11 (1), e0358622.
Weng, K.F., Chen, L.L., Huang, P.N., Shih, S.R., 2010. Neural pathogenesis of enterovirus 71 infection. Microbes. Infect. 12 (7), 505–510.
Yi, E.J., Shin, Y.J., Kim, J.H., Kim, T.G., Chang, S.Y., 2017. Enterovirus 71 infection and vaccines. Clin. Exp. Vaccine Res. 6 (1), 4–14.
Yogarajah, T., Ong, K.C., Perera, D., Wong, K.T., 2017. AIM2 Inflammasome-mediated pyroptosis in enterovirus a71-infected neuronal cells restricts viral replication. Sci. Rep. 7 (1), 5845.
Yu, P., Zhang, X., Liu, N., Tang, L., Peng, C., Chen, X., 2021. Pyroptosis: mechanisms and diseases. Signal Transduct. Target Ther. 6 (1), 128.
Zhang, W., Huang, Z., Huang, M., Zeng, J., 2020. Predicting Severe Enterovirus 71-Infected Hand, Foot, and Mouth Disease: cytokines and Chemokines. Mediat. Inflamm. 2020, 9273241.
Zhang, X., Hao, J., Sun, C., Du, J., Han, Q., Li, Q., 2022. Total astragalosides decrease apoptosis and pyroptosis by inhibiting enterovirus 71 replication in gastric epithelial cells. Exp. Ther. Med. 23 (3), 237.
Zhang, Y.J., Zhu, W.K., Qi, F.Y., Che, F.Y., 2023. CircHIPK3 promotes neuroinflammation through regulation of the miR-124-3p/STAT3/NLRP3 signaling pathway in Parkinson's disease. Adv. Clin. Exp. Med. 32 (3), 315–329.
Zhao, Z., Li, Q., Ashraf, U., Yang, M., Zhu, W., Gu, J., Chen, Z., Gu, C., Si, Y., Cao, S., Ye, J., 2022. Zika virus causes placental pyroptosis and associated adverse fetal outcomes by activating GSDME. Elife 11.
Zhou, W.Y., Cai, Z.R., Liu, J., Wang, D.S., Ju, H.Q., Xu, R.H., 2020. Circular RNA: metabolism, functions and interactions with proteins. Mol. Cancer 19 (1), 172.